

Molecular Rheology and Statistics of Long Chain Branched Metallocene-Catalyzed Polyolefins

D. J. Read*[†] and T. C. B. McLeish[‡]

Department of Applied Mathematics, University of Leeds, Leeds, LS2 9JT, U.K.; and IRC in Polymer Science and Technology, Department of Physics and Astronomy, University of Leeds, Leeds LS2 9JT, U.K.

Received August 25, 2000; Revised Manuscript Received December 6, 2000

ABSTRACT: We derive the rheologically relevant “priority” and “seniority” distributions of entangled segment topology from a kinetic model of long chain branch formation in metallocene-catalyzed polyolefins. For the model considered, the chemistry results in a two-parameter family of molecular distributions; convenient parameters are the typical strand molecular weight between cross-links and a branching probability. Only the branching probability controls the chain topologies. We comment on the different nature of the metallocene ensemble from the usual gelation ensemble that is a candidate model for standard low-density polyethylene. We calculate the extensional rheology of a model system within a decoupling approximation that permits a partial mapping onto the “multimode pom-pom” constitutive scheme.

1. Introduction

The remarkable rheological properties of entangled polymer melts and solutions have continued to fascinate the polymer science community since the key developments of synthetic routes to monodisperse model polymers¹ and powerful molecular theories for melt dynamics. The most successful of these are based on the tube model of entanglements.² Particularly notable have been the advances in understanding the effect of long chain branching (LCB) as it has long been known that, together with the molecular weight itself, this aspect of molecular topology is the most sensitive controlling feature of the melt rheology. The long-term goal is a quantitative theory for the rheological response of a statistical melt of known polymerization kinetics, particularly as control of molecular topology is becoming a reality even at the industrial scale.³

The highly processable polymer low-density polyethylene (LDPE) is the best-known case, enhanced by its strong “melt strength” in processing flows that arises from extension hardening.⁴ However, the detailed branched structure of LDPE is conjectured but not known in detail, and experimental anionic molecular architectures of small polydispersity have been essential to work with until now because they alone have provided quantitative tests for molecular rheological theories. For example, they have checked the very different predictions given by the tube model for entangled dynamics in the two cases of linear^{5,6} and star-shaped^{7–9} chains. Modeling the topological restrictions on a given chain from its neighbors as a confining tube of diameter a (of a size specific to each chemistry) along the chain contour, linear chains renew their configurations chiefly by a curvilinear diffusion called reptation. This leads to the prediction of a near single-exponential form of the relaxation modulus $G(t)$ and a dependence of the relaxation time τ_{rep} on molecular weight of $M^{\beta,4}$, when account has been taken of path length fluctuations.¹⁰ Star polymers, however, are forbidden the reptation

route, and must rely solely on the successively more unlikely path length fluctuations to renew configurations of chain segments nearer and nearer to their branch points. Now a very broad range of relaxation times is predicted, corresponding to the different distances of segments from the free ends. The longest relaxation time (of the segments nearest the branch points) have an exponential dependence on the arm molecular weight. Both of these features are borne out by experiments on anionically polymerized monodisperse star and linear melts of different chemistries. Of particular note is the initially surprising independence of the viscosity on the number of arms of a star polymer (unless this is very large).

Recently the tube model theory for star polymers¹¹ has been extended to blends of star-with-star¹² and star-with-linear¹³ polymers and to the next most complex topology of branched polymer, the H-architecture.^{14–16} The quantitative success of the model in these cases is all the more remarkable in face of the small number (two) of free parameters (the plateau modulus G_0 and a monomeric friction constant or equivalently the Rouse time of an entanglement length τ_e). These are furthermore constrained to be consistent with literature values obtained from linear polymers for each local chemistry. A natural consequence of the theory is the universality of melt rheology of flexible polymers providing all molecular weights are expressed in terms of the entanglement molecular weight M_e . Values of M_e specific to many different chemistries are now available.¹⁷ Nonlinear rheology is also predicted essentially without additional parameters. For example the “damping functions” of LCB polymers (the factorable dependence on strain in a nonlinear shear step-strain experiment) are not as shear-thinning as those of linear polymers.¹⁸ It might have been expected that such novel properties of branched polymers in nonlinear flows would be seen in the simplest case of monodisperse star polymers. However, they seem to be just as shear-thinning as linear melts, following a Doi–Edwards damping function,⁹ at least in step shear. Within the framework of tube model this is not a surprise because the strong reduction of

[†] Department of Applied Mathematics, University of Leeds.

[‡] Department of Physics and Astronomy, University of Leeds.

stress on large strains is explained by the rapid retraction of chains within strained (and so extended) tubes. Such a retraction is clearly not hindered in the case of star polymer melts because of the high curvilinear mobility of the free ends. In star polymers, every piece of chain segment is topologically connected directly to a chain end and so may retract as rapidly within its tube as a linear chain. This is not the case for the next most complex topology of branched polymer, the H-architecture.^{14,15} H-polymers have four starlike arms, which must relax by path length fluctuation in linear response, and are indeed free to retract rapidly after large strains. But they are connected by a “crossbar”, a novel type of chain segment trapped between branch points. Under large strains, they are not free to retract rapidly (but see below for very high strains), so suggesting qualitatively new dynamical behavior in this case. Yet at long time scales, when the dangling arms have completely relaxed, these slow central sections must behave as linear polymers (by “dynamic dilution”). So the H-polymer combines an intriguing combination of the features of star and linear polymers in linear response while exhibiting a radical departure from both structures in nonlinear response.¹⁶ It shares this property with all comblike structures,^{19,20} of which it is the simplest member.

A generalization of the H-structure called “pompoms”, in which an arbitrary number of long branches are attached to each end of the crossbar, has recently been developed into a rather general constitutive framework for branched polymers.²¹ Capturing the essential insight that the entanglement structure of a melt separates the relaxation times of segment stretch and orientation, it permits variation of the “degree of branching” also. More remarkably, an uncoupled polydisperse ensemble of model “pompom” molecules possesses a linear and nonlinear rheological response that can be very closely matched to all known data on published LDPE grades.^{22,23} It seems possible to map a complex topological mix onto a rheologically equivalent set of pompom modes for many practical purposes. This suggests that the mechanical coupling between the levels of random entangled treelike polymers may be a second order effect: each pompom mode somehow captures the rheological contribution of segments at a typical “depth” (we refine this notion in the next section) and consequent relaxation time for stretch and orientation. Ideally, we would like to be able to predict the relevant weights and orientation times from the molecular architecture directly.

An opportunity to do this is provided from recent advances in metallocene catalysis that allow the placement of long-chain branches on commercial polyolefins in a controlled way.²⁴ For example, the clean reaction scheme of vinyl re-incorporation has permitted *ab initio* calculations of the bivariate distribution of molecular weight and number of long chain branches.²⁵ Yet LCB metallocene polyethylenes share with the less well-defined LDPE the property of extension hardening, apparent damping functions much less shear-thinning than those of linear polymers, and at the molecular level a wide variety of possible structures.

We show in this paper how the statistical calculations of the LCB metallocene reaction scheme may be extended to the rheologically relevant statistics of segment topological “depth”, and how a distribution of rheological

relaxation times and strain-hardening parameters may be calculated from them. In the next section, we review the current understanding of these proper statistical functions required to calculate rheological response from a melt of LCB-entangled polymers. Then we review the minimal model for the metallocene reaction chemistry before the calculation of the rheological statistics. Finally we calculate linear and nonlinear extensional rheological response of a model LCB polymer in a decoupling approximation that maps the topological statistics onto a pompom ensemble.

2. Rheologically Relevant Statistics for LCB Polymers

Work on model branched polymers over the last 10 years has identified two important topological properties of segments belonging to LCB melts.⁸ The “seniority” distribution controls the linear rheological response, while the “priority” distribution limits locally the allowed segmental stretch, and so controls nonlinear properties such as the damping function in strong step shear, and strain hardening in extension. We review their underlying physics and properties briefly in this section.

2.1. Seniority. In entangled branched polymers, the principal mechanism of a segment’s orientational relaxation is the escape from its tube constraints via retraction of a free chain end into the tube. This replaces the simple curvilinear reptation of linear polymers, which is suppressed by the highly immobile branch points. Retraction also induces a completely different pattern and distribution of stress relaxation within the entangled polymers, for the critical first-passage times of a chain end through tube segments begin small at the molecule’s extremities but become exponentially large toward the center. This is because the retraction occurs against an entropic elastic potential that serves to keep entangled chain closely to a mean curvilinear density along the tube.² The simplest example is the star polymer melt, in which is obtained the stress relaxation time $\tau(x)$ of a tube segment a fractional distance x from a chain end. This time corresponds to arm retraction as far as the segment itself, and is given approximately by

$$\tau(x) = \tau_0 \exp\left(\frac{15M_a}{4M_e} \left[\frac{x^2}{2} - \frac{x^3}{3}\right]\right) \quad (1)$$

where τ_0 is an attempt time for arm retractions. The important multiplying factor of the number of entanglements in the star arm M_a/M_e is determined by allowing previously relaxed segments from surrounding star arms to dilute the tube constraints for all slower segments. This “dynamic dilution” is essential to account quantitatively for experiments on monodisperse star polymers¹¹ and in more detailed calculations permits further refinements of the dependence of τ_0 on M_a .

Generalizing the tube model to highly branched architectures leads to a generalized segment “depth” from the topological exterior of a molecule, which has been dubbed the “seniority” m . This number, a property of an interior segment of a branched molecule, is simply the number of segments (chain portions between branch points) that connects it to the retracting chain end responsible for its relaxation. Stress relaxation occurs hierarchically in segment seniority: when all outer (seniority = 1) segments have relaxed as arms of star polymers (albeit in the presence of much slower mate-

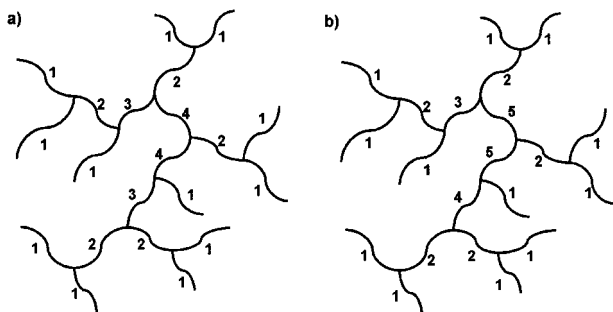


Figure 1. Branched polymer, with chains between branches labeled with the topological numbers relevant to rheology. (a) Seniority: To calculate this for a given segment, count the number of strands to the furthest chain end on each side of the segments, then take the smaller of the two values. (b) Priority: To calculate this for a given segment, count the number of chain ends attached to each side of the strand, and then take the smaller of the two values.

rial), the seniority = 2 segments can begin relaxation in a similar way. They, too, behave like retracting star arms because, on the time scales of their own dynamics, the seniority = 1 segments are rapidly and continually reconfiguring and do not contribute to the entanglement environment. The only distinction is that all the effective drag on any currently relaxing segment is imposed on its exterior end, arising from the dissipation from lower seniority segments attached there. The effective tube diameter also increases with seniority. Since the effective entanglement molecular weight M_e dilutes with polymer concentration as²⁶ $M_e \sim c^{-\alpha}$, with $\alpha = 4/3$, the time scale for the relaxation of each seniority is recursively dependent on the previous one via an exponential term similar to that in a simple star polymer

$$\tau(m+1) = \tau(m) \exp\left(\frac{15}{8} \frac{M_x}{M_e} [S(m)]^\alpha\right) \quad (2)$$

where M_x is now the molecular weight between branch points, assumed constant. So all that is required to calculate the relaxation time distribution within this discretized approximation (applicable for high levels of branching) is the concentration of unrelaxed segments $S(m)$ at seniority m . Evidently the volume fraction of segments of seniority m itself is just $s(m) = S(m-1) - S(m) \approx -dS/dm$ (for large m). Two extreme cases are pertinent: the regular ‘‘Cayley Tree’’ melt in which $S(m) \sim e^{-\gamma m}$, with γ depending on the functionality of the lattice,²⁷ and the case of random branching close to the gelation-point limit, where²⁸ $S(m) \sim m^{-2}$. In the latter case the calculation of seniority is subtle, even with so coarse an approximation as monodisperse molecular weights between branch points: a segment may be released by retraction from the subcluster on either end of it, whichever is faster. However, within this subcluster it will be the longest path to the exterior that determines the retraction time. As an example, this recipe is used to annotate the seniority to each segment in the representative molecule in Figure 1a.

In this, and in all statistically generated ensembles of branched polymers, the solution of the dynamic-dilution equation (eq 2) should be sought without explicit enumeration of architectures if at all possible. In these cases, and in the metallocene case below, this is possible, and analytic forms are obtained.

As a final step in calculating the linear rheology, the relaxation spectrum $G(t)$ counts contributions from all

seniorities at their appropriate time scales, which in a continuous approximation becomes

$$G(t) = \int_1^\infty \frac{dG(S(m))}{dm} e^{-t/\tau(m)} dm = G_0(\alpha + 1) \int_1^\infty [S(m)]^\alpha s(m) e^{-t/\tau(m)} dm \quad (3)$$

2.2. Priority. For small nonlinear strains, the branch points in a LCB melt will move affinely just as crosslinks of a deforming network would. If continued to high strains this would lead to indefinitely high extension-hardening as all segments are stretched by the flow. But of course LCB melts are not networks, and the extension hardening is limited. Strong evidence has emerged that traces the upper limit of extension hardening to a molecular process we have called ‘‘branch point withdrawal’’. This is most clearly seen in the H-shaped structure: at equilibrium each segment of entangled polymer chain carries a ‘‘Brownian tension’’ force of $3k_B T/a$ along its contour. After a step strain, the outer arms of the H-polymer quickly relax their increased path length and tension back to equilibrium values,¹⁶ but this cannot happen for the segment trapped between the branch points, whose tension increases proportionally to its contour length (it behaves as a Gaussian chain). When this contour length has increased to beyond twice its equilibrium length, the curvilinear tension it supports becomes greater than twice the equilibrium value, yet this is just the force on the branch point supplied by the two outer arms together. Beyond this point the central segment can be stretched no further, however great the deformation of the surrounding melt. By simple extension of this argument, the ‘‘pompon’’ generalization of the H-structure, with q arms attached on each end of the central segment, permits extension to exactly $k = q$ times the equilibrium contour length before branch point withdrawal. We call k the ‘‘priority’’ of the central segment. In the constitutive behavior of these model molecules it directly determines the limit of extension hardening,²¹ and in experiments the limit of a stable fiber extension.¹⁶

The generalization of priority to multiply branched polymers has been examined, like the seniority statistic, in the cases of both regular Cayley trees and the mean-field gelation ensemble.²⁹ Strand tensions propagate from the exterior of the molecule so that immediately after a step strain the maximum extension of any strand (its priority) is just the number of exterior strands to which it is connected on the end that suffers branch point withdrawal first. In the case of the Cayley tree this is just $k = z^p$ where z is the functionality of the lattice and p is the level of the segment counting from the exterior (p is also the seniority in this highly symmetric case). The number of such segments is of course exponentially smaller as p increases. For randomly branched polymers, the calculation of the priority distribution is performed from its recursive definition via a generating function²⁹ (we will employ this tactic again below). Remarkably, in both these cases the weight of priorities $P(k) \sim k^{-2}$ in the continuum approximation. The recipe for calculating segment priority is illustrated in the case of a single molecule in Figure 1b.

In a constitutive scheme that counts the stress contribution from each segment of a melt, the segment priority will be used, just as in the pompon model to limit the maximum extensions in an arbitrary flow. A

useful approximation in estimating critical strains for maximum extensions in steady flows or large step strains is that the mean extension of a random walk embedded in an affinely deforming medium extends by $1/2$ the principal strain, so that a segment of priority k will extend no further in a step strain whose magnitude exceeds $2k$.

2.3. Bivariate Distributions. We have motivated an approximation for the molecular rheology of a complex LCB melt in which the orientational relaxation times of segments are calculated from their seniority, and their maximum extensions from their priority. In all entangled fluids it is vital to recognize the separation of the time scales of stretch, $\tau_s(m)$ and orientational relaxation, $\tau_b(m)$ of each entanglement segment,²¹ but in a multiple-seniority melt, the stretch relaxation must additionally be bounded above by its own orientational relaxation and below by the orientational relaxation time of the next lower seniority. In practice, this sets well-controlled bounds on the stretch relaxation times of segments.²² So at first sight, the bivariate distribution of priorities and seniorities $w(k,m)$ seems sufficient to set up a constitutive equation for the melt in which each seniority and priority fraction is mapped onto a pom-pom rheological element²¹ with the corresponding relaxation times for orientation and stretch, and a maximum stretch of k .

A further level of treatment suggests itself, however, when the huge separation of time scales in LCB melts is contemplated. An imposed flow rate of $\dot{\gamma}$, say, sets a natural time scale of $\tau \sim 1/\dot{\gamma}$ on the melt. Because of the exponentially large range of time scales of relaxation spanning segments of low and high seniority, this time scale will typically divide the segment distribution into two classes; those with relaxation times much faster than τ , which reconfigure rapidly on the time scale of the flow, and those with relaxation times much slower than τ , which are strongly affected by the flow. It is only the second class of segments that form the effective entanglement network of the fluid and contribute to the stress beyond a simple Newtonian response. Essentially, this ensemble, consisting only of unrelaxed segments at $\tau \sim 1/\dot{\gamma}$, has a different topology from the full (high frequency) case and is effectively less branched. Again the simplest example of this topological renormalization with time scale is the H-polymer. At time scales longer than the arm relaxation time, only the linear crossbar segments contribute to the viscoelasticity. These relax stress by reptating in tubes created by other crossbars only, and behave as if they had priority 1, even though they possess priority 2 at short time scales.¹⁶

Of course a full theoretical treatment of multiply branched polymers will capture this renormalization naturally as outer segments relax their stress. It is after all the sum of the actual tensions from all outer segments on the terminating branch point of an inner segment that gives its (time-dependent) maximum stretch.³⁰ At the level of approximate rheological response discussed here, we will be content with an approximation that selects a fixed time scale for the flow, then calculates the effective bivariate seniority and priority distribution for that time scale. The effective molecular ensemble is constructed from the full chemical one by “snipping” away all outer segments until we first find a seniority that is in marginally nonlinear response (e.g., Figure 2). The minimal distribution that captures all this physics even at the level of a seniority-

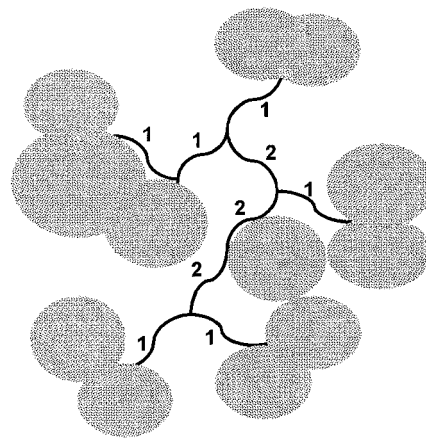


Figure 2. Same branched polymer as in Figure 1, but at a time scale where the outer arms are relaxed (i.e., “snipped”). The numbers shown are the effective values of the priority at this time scale.

decoupled approximation is therefore the trivariate function $\tilde{w}(k,m,n)$. This is the weight of segments of priority k and seniority m in an ensemble whose outer seniorities have been removed by dynamic dilution to seniority n . In the final section, we write down the explicit connection between this statistic and the multimode pom-pom constitutive approximation we use but now return to the calculation of this and simple statistics for the LCB metallocene ensemble.

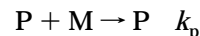
3. Reaction Chemistry for LCB Formation

To make detailed calculations of any statistics for the ensemble of polymers in a reaction bath, we must consider the details of the reaction chemistry. In particular, we must examine the effect of the chemistry on the shapes of polymers formed.

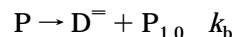
In this paper, we assume (for the purposes of clarity) a slightly simplified version of the reaction chemistry described by Soares and Hamielec²⁵ for the formation of long chain branched PE via single-site metallocene catalysis. The reaction is illustrated in Figure 3. For a chain growing at a catalyst site, there are four possible reactions, represented schematically as follows:

In the first reaction, a monomer (M) is added to a

1. Monomer addition



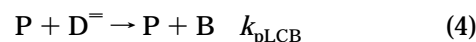
2. Chain transfer to double bond



3. Chain transfer to dead chain



4. Long-chain branch formation



“living” chain at a catalyst site (P). The resulting chain remains attached to the catalyst, and so retains the label P for a living chain (we can add subscripts later, for example to denote that the degree of polymerization has increased by one).

In the second reaction, the living chain detaches from the catalyst site so that it now terminates with a double bond (denoted by D^{\equiv}). Such a detached chain may take

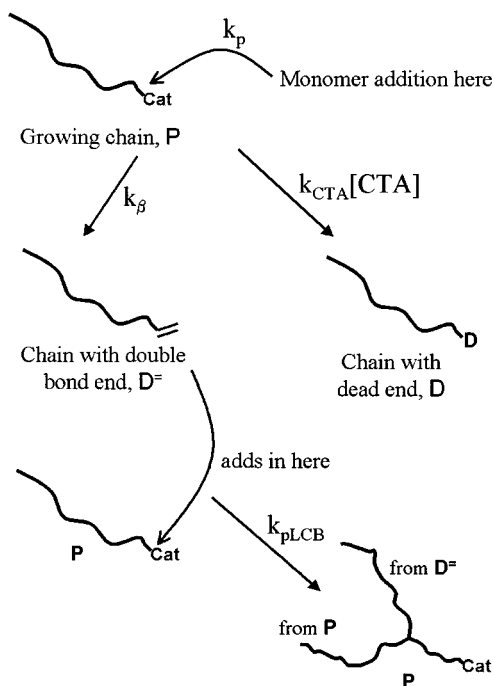


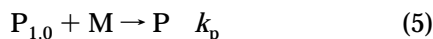
Figure 3. Schematic diagram of the reaction mechanism for long chain branch formation with single-site metallocene catalysts.

part later in LCB formation. The detached chain leaves behind a single monomer attached to the catalyst site, denoted by $P_{1,0}$. We retain the notation of Soares and Hamielec,²⁵ wherein the subscript 1,0 refers to a living chain comprising one monomer and no branches. In the analysis below, the $P_{1,0}$ species will be considered as distinct from the living chain population, P .

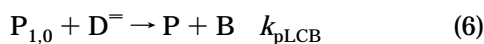
In the third reaction, a chain transfer agent (CTA) prompts the detachment of a living chain from the catalyst site, with the production of a $P_{1,0}$ species and a "dead" chain (D). The dead chain plays no further part in the reaction.

The fourth reaction results in the formation of a long chain branch. Instead of incorporating a monomer into the chain, a living chain (P) reacts with a chain ending in a double bond ($D^=$) produced in the second reaction. The result is a living chain (P) containing an extra branch point (labeled B).

For the $P_{1,0}$ species, we include only one reaction, in which a monomer is added to form the start of a living chain:



This reaction is effectively an initiation step for the living chains. Soares and Hamielec²⁵ also explicitly included a "long chain branching" reaction for the $P_{1,0}$, which takes the form



While it is possible for us to include this reaction in the development that follows, it detracts from the clarity of presentation without significantly affecting the physics. We also note that chain transfer reactions for $P_{1,0}$ similar to reactions 2 and 3 above are implicit in some of the mathematical development of Soares and Hamielec.²⁵ The precise chemical details of reactions such as initiation and chain transfer affect the overall

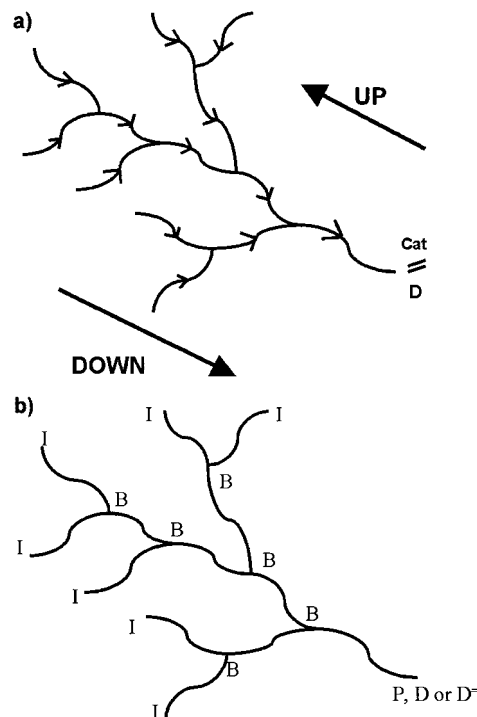


Figure 4. Typical shapes of long chain branched polymers made via the mechanism of Figure 3. (a) The direction of the arrows indicate the direction of polymer growth, which is conserved in all branching reactions. This allows the labeling of the directions "upstream" and "downstream". (b) Labeling of the molecule with sites for "initiation" (I), "branching" (B), and "termination" (P, D, or $D^=$). The reactor concentrations of such sites allow the definition of branching probabilities.

concentration of various species in the reactor bath, but do not affect the typical structure of the molecules formed, nor the nature of the calculation used to enumerate the structures. For example, in Appendix B, we obtain a distribution of molecular weight and number of branches which is identical to that of Soares and Hamielec.²⁵

3.1. Qualitative Description of the Chain Structure. From the reaction illustrated in Figure 3 and discussed above, it is clear that all polymer chains in the reaction mixture have a typical shape, illustrated in Figure 4a. Each chain contains just one unique free end attached to either a catalyst site (P chains) a double bond ($D^=$ chains) or a dead end (D chains). All other free ends in the molecule were produced in an initiation step, eq 5. It is therefore possible to draw an arrow on each polymer strand between cross-links, pointing along the molecule toward the unique free end. This arrow represents the direction in which monomers were added to the polymer molecule, the growth direction. This direction is preserved during all the above reactions, notably during the formation of long-chain branches (the directions of the arrows on the reacting P and a $D^=$ species remain the same in the resulting P species). In the development that follows, we shall call the molecular direction along the arrows *downstream* and the opposite direction *upstream*.

This "directionality" of the polymer chains is fundamental to the metallocene reaction chemistry. We shall later show that the statistics of the polymer chains are different in the downstream and upstream directions. This fact can be seen qualitatively by the fact that at every branchpoint in the molecule, two arrows point inward and a single arrow points outward, representing

the fact that each time a branchpoint is formed two molecules are combined to form a single chain.

3.2. Detailed Balance in a Steady-State CSTR. We now make the further assumption that the polymerization reaction is performed in a steady-state continuous stirred tank reactor, which is typical for metallocene LCB reactions. In the idealization of this, it is assumed that the concentration of reagents varies neither in time nor space within the reaction vessel. This allows us to write down detailed balance equations for each reagent as follows.

We denote with a subscript the concentration of a specific fraction x of a species (x might be degree of polymerization or number of branchpoints). For example, P_x is the (number) concentration of P species with property x . The total concentration of a given species is denoted without a subscript, so (for example) $P = \sum_x P_x$. We can write detailed balance equations for the whole concentration of a species, or fraction by fraction.

From eqs 4 and 5, the rate equations for P and $P_{1,0}$ are

$$\frac{dP}{dt} = -sP - k_{\text{CTA}}[\text{CTA}]P - k_{\beta}P + k_pMP_{1,0} \quad (7)$$

$$\frac{dP_{1,0}}{dt} = -sP_{1,0} + k_{\text{CTA}}[\text{CTA}]P + k_{\beta}P - k_pMP_{1,0} + \text{feed} \quad (8)$$

where s is the inverse of the mean residence time, and "feed" represents the input of reagents into the reactor (including initiation steps for the $P_{1,0}$). Since we are in a steady state, the time derivatives may be set to zero, and we obtain two equations for P and $P_{1,0}$ which are equivalent only if

$$\text{feed} = sP + sP_{1,0} \quad (9)$$

The interpretation is that the rate at which living polymer is convected out of the reaction vessel is matched by the input of fresh catalyst and initiator. In this steady-state condition, P and $P_{1,0}$ are related by

$$P_{1,0} = \frac{P(s + K_T)}{k_pM} \quad (10)$$

where $K_T = k_{\beta} + k_{\text{CTA}}[\text{CTA}]$.

The rate equations for each fraction of the double bond and dead species are

$$\frac{dD_x^=}{dt} = k_{\beta}P_x - k_{\text{pLCB}}PD_x^= - sD_x^= \quad (11)$$

$$\frac{dD_x}{dt} = k_{\text{CTA}}[\text{CTA}]P_x - sD_x \quad (12)$$

Again setting time derivatives to zero, we obtain

$$D_x^= = \frac{k_{\beta}P_x}{k_{\text{pLCB}}P + s} \quad (13)$$

$$D_x = \frac{k_{\text{CTA}}[\text{CTA}]P_x}{s} \quad (14)$$

These last two equations are true both fraction by fraction (i.e., with subscripts) and for the population of

each species as a whole. It follows that the probability distribution of $D_x^=$ and D_x with respect to any variable, x (for example, the molecular weight distribution) is identical to that of the living polymers, P_x . In other words, *the statistical distribution of the living, dead, and double bond chain species are identical*.^{12,4,25}

We can also obtain an expression for the concentration of branchpoints, B , in the reactor vessel, which will be of use later. The rate equation is

$$\frac{dB}{dt} = k_{\text{pLCB}}PD^= - sB \quad (15)$$

giving

$$B = \frac{k_{\text{pLCB}}PD^=}{s} \quad (16)$$

3.3. Branching probabilities. In the above section, we demonstrated that, under steady-state conditions, the statistical distribution of the living, dead and double bond polymer species were identical. If we now consider the long-chain branching reaction, we note that it combines a P species and a $D^=$ species. Each of these species is taken from an identical statistical distribution. The resulting chain, a P species, must be part of that same statistical distribution. It therefore follows that the statistics of each of the subbranches of the new chain must have identical statistics to the chain as a whole. Furthermore, since this is true of every branch-forming reaction, it follows that *the statistical properties of every sub-branch on every chain are identical to the statistics of the whole chains*. The molecules formed in steady-state conditions are self-similar.

In the following sections, we shall proceed to calculate the statistical distribution of rheologically relevant parameters for the ensemble of polymers in the reaction mixture. To achieve this, we shall make use of the self-similarity of the polymer chains, via branching probabilities defined as follows. If we pick a polymer strand at random from the reaction mixture, then the probability of hitting a branch point (as opposed to a chain end) by stepping along the chain is b^U for the upstream direction, and b^D for the downstream direction. These probabilities may be calculated from the concentrations of reactive species derived above through the detailed balance equations.

We note that, for any of the polymer chains in the reaction bath, there is a single free end with a double bond, dead end or catalyst attached. All other free ends were produced in initiation steps, and the total number of these initiation (I) sites on a given chain is just the number of branchpoints, plus one. All chains are of the form shown in Figure 4b. Therefore, the total concentration of initiation sites in the reaction bath is simply

$$I = B + P + D^= + D \quad (17)$$

The upstream branching probability is simply the total number of strands which hit a branchpoint upstream (B), divided by the total number of strands ($B + I$, since all strands either hit a branchpoint or an initiation site upstream).

$$b^U = \frac{B}{B + I} = \frac{B}{2B + P + D^= + D} \quad (18)$$

The downstream branching probability is the total number of strands which hit a branch downstream ($2B$, since all branchpoints have two strands hitting them from upstream), divided by the total number of strands.

$$b^D = \frac{2B}{2B + P + D^{\overline{}} + D} \quad (19)$$

We note that b^U and b^D are related by

$$b^D = 2b^U \quad (20)$$

which implies $b^U \leq 1/2$. The limit $b^U = 1/2$ is, in fact, the percolation threshold, as will become apparent in the following.

Using these branching probabilities, it is possible to calculate the bivariate distribution of molecular weight and number of branchpoints per molecule, a distribution calculated by Soares and Hamielec, using a different method.^{24,25} We show our derivation of this distribution in Appendix B. At this point we simply note that, as far as the topology of the ensemble of branched polymers is concerned, this reaction scheme contains *only one parameter, b^U* ! All reaction rates and reactant concentrations affect the ensemble only through this number. The exponential functions in the bivariate distributions of Appendix B additionally indicate that only one other parameter (the mean degree of polymerization between branch points, N_x , is a convenient choice) is sufficient to specify both the topological and mass distributions of the entire ensemble. In what follows, we shall use the branching probability, rather than reactor concentrations, as the fundamental variable. We note that b^U is related to the reactor variables via

$$b^U = \frac{k_\beta k_{\text{PLCB}} P}{(2k_\beta + k_{\text{CTA}}[\text{CTA}] + s)k_{\text{PLCB}} P + (k_\beta + k_{\text{CTA}}[\text{CTA}] + s)s} \quad (21)$$

As shown in Appendix B, the mean degree of polymerization between branch points is related to the reactor variables via

$$N_x = \frac{1}{\ln A} \quad A = \frac{k_p M}{k_p M + k_{\text{CTA}}[\text{CTA}] + k_\beta + k_{\text{PLCB}} D^{\overline{}} + s} \quad (22)$$

Appendix B also gives some useful relationships between the parameters b^U and N_x and various molecular weight averages of the distribution.

4. Quantitative Chain Statistics for Rheological Calculations

Having established a description of the molecular shapes obtained from the metallocene long chain branching reaction, we now aim to calculate statistics of the rheologically relevant variables, seniority and priority. Ultimately, as suggested in section 2.3, the goal is to calculate the distribution $\tilde{w}_{k,m,n}$ of chain segments with “snipped” priority k and seniority m at a flow time scale such that all segments up to seniority n have already relaxed. We begin by calculating the individual priority and seniority distributions, before calculating the full

bivariate distribution. The calculation without snipping will be presented in the text; we restrict the more involved calculations with snipping to Appendix A.

4.1. The Seniority Distribution. The seniority of a given polymer strand may be evaluated by counting the number of strands to the furthest free end in each direction (inclusive of the current strand, so the minimum seniority is 1). The seniority is then the smaller of the two values. Here as discussed in section 1, we are making a “monodisperse strand” approximation. In other words we assume a one-to-one correspondence between the seniority of a segment and its orientational relaxation time by path length fluctuation. This would arise from the dynamic dilution eq 2, by inspection, only if all strands between branch points were of some fixed molecular weight M_x . In reality the exponential distribution of molecular weights between branch points will blur the one-to-one correspondence between seniority and relaxation time, but in a highly branched ensemble, this will self-average along a retracting path to a high degree. [Other, purely topological, inhomogeneities also do this, but we defer a more refined treatment of the relation between seniority and relaxation time to future work.] To see how this works consider the highly branched limit in which concentration of the entanglement network $S(m)$ is changing slowly with seniority. Then, from eq 2, the change in $\log \tau(m)$ between $m = m'$ and $m = m' + p$ on a single molecular branch, is proportional to the sum $M_{x,m'} + M_{x,m'+1} + \dots + M_{x,m'+p}$, where $M_{x,i}$ is the molecular weight of the strand on that branch of seniority i . If all of these molecular weights are chosen randomly from an exponentially distributed ensemble, then the standard deviation of the sum is $\sqrt{pM_x}$ as compared to an expectation value for the sum of pM_x . So on the scale of $\log \tau$ (which is standard for presentation of rheological data) short sections are usually balanced by longer sections on the same branch. Even in cases of low branching, rheological response at very long times and with high seniority must arise from retracting chains containing many branch points, although these are untypical for the ensemble as a whole. So here, too, the monodisperse strand approximation is not expected to give wildly inaccurate predictions, though clearly needs to be addressed in future work. Moreover, the approximation is of the same order as the decoupling approximation we are going to make in calculation of the rheology in section 5 below, so we choose to proceed with it at this point.

It is convenient first to calculate the two “single-sided” distributions (i.e., the distance to the furthest free end upstream and downstream) before combining them to form the “bidirectional” distribution of seniorities found from the smaller of the upstream and downstream seniorities. We proceed by calculating the cumulative seniority distribution, defined upstream as

$$f_m^U = P(\text{upstream seniority} \leq m) \quad (23)$$

The probability s_m^U of seniority m is then given by

$$s_m^U = f_m^U - f_{m-1}^U \quad (24)$$

The upstream cumulative seniority may be calculated by noting that a strand chosen at random will either be unbranched (seniority 1, which is $\leq m$, with probability $1 - b^U$), or will be branched, with probability b^U .

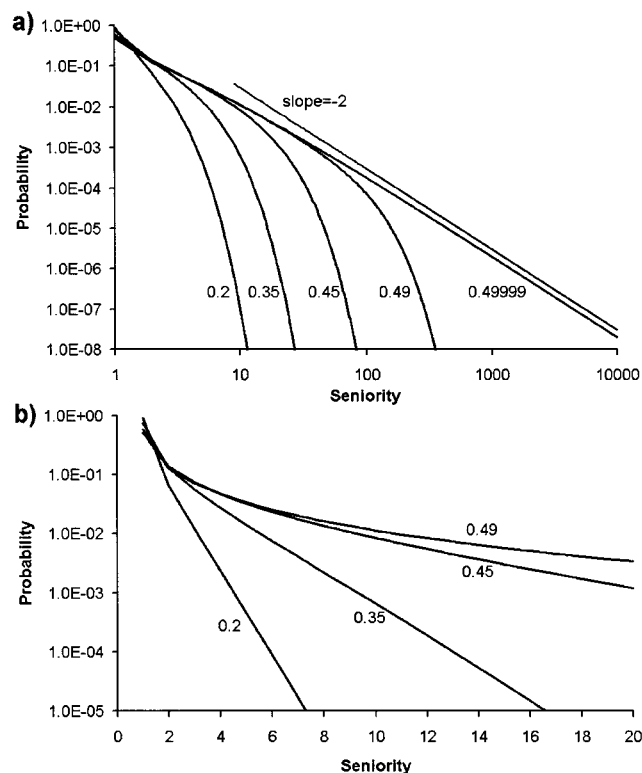


Figure 5. Seniority distribution s_m for different values of the branching parameter, $b^U = 0.2, 0.35, 0.45, 0.49, 0.49999$ on (a) a log–log scale and (b) a linear–log scale. There is a crossover between exponential decay and power-law dominated behavior—the power law dominates for lower seniorities and close to the percolation threshold.

If it is branched, then it has seniority $\leq m$ only if the subsequent two strands have seniority $\leq m - 1$. Hence

$$f_m^U = (1 - b^U) + b^U [f_{m-1}^U]^2 \quad (25)$$

This is a recursive formula which can be used to generate all the f_m^U by noting that $f_1^U = (1 - b^U)$. Similarly, downstream

$$f_m^D = (1 - b^D) + b^D f_{m-1}^U f_{m-1}^D \quad (26)$$

with $f_1^D = (1 - b^D)$. We have used the fact that there is one upstream and one downstream strand after a downstream branchpoint.

Having obtained the cumulative probability distributions f_m^U and f_m^D we can obtain the bidirectional seniority distribution. Since a chain segment relaxes by the fastest route available, the bidirectional seniority is the smaller of the upstream and downstream seniorities. Hence, a bidirectional seniority of m is obtained when the upstream seniority equals m and the downstream seniority $> m$, or when the downstream seniority equals m and the upstream seniority $> m$, or when both equal m . In terms of probabilities, this reads

$$s_m^B = s_m^U (1 - f_m^D) + s_m^D (1 - f_m^U) + s_m^U s_m^D \quad (27)$$

This seniority distribution is shown for various values of the branching parameter b^U in Figure 5.

4.1.1. Relaxation Times near the Percolation Threshold. The metallocene ensemble can approach the percolation threshold of $b^U = 1/2$ but not cross it.

We now examine the scaling behavior of the seniority distribution near this threshold. To do this, we define the complement of the cumulative upstream seniority distribution

$$S_m^U = P(\text{upstream seniority} > m) = 1 - f_m^U \quad (28)$$

S_m^U is the unrelaxed concentration at time scale corresponding to seniority, m . Substituting into eq 25 gives

$$S_{m+1}^U - S_m^U = -(1 - 2b^U) S_m^U - b^U (S_m^U)^2 \quad (29)$$

and taking the large m limit, we can replace $S_{m+1}^U - S_m^U$ with dS_m^U/dm to give a differential equation with two distinct regimes near percolation (i.e., when $(1 - 2b^U)$ is small). In the limit of very small S_m^U where $(1 - 2b^U) \gg b^U S_m^U$ the first term on the right-hand side of the equation dominates. The solution in this regime is an exponential decay:

$$S_m^U \sim \exp[-(1 - 2b^U)m] \quad (30)$$

For larger S_m^U where $(1 - 2b^U) \ll b^U S_m^U$, the second term in the differential equation dominates, and

$$S_m^U \sim m^{-1} \quad (31)$$

$$s_m^U = -\frac{dS_m^U}{dm} \sim m^{-2} \quad (32)$$

Near percolation, then, the upstream seniority distribution gives a power law as above, with an exponential cutoff at high m .

Downstream, we note that at percolation, $b^D = 1$, so the first term on the RHS of eq 26 is always zero. The only solution is $f_m^D = 0$, and hence, $S_m^D = 1$ for all m . The molecule is effectively infinite downstream, so that the bidirectional seniority distribution (which always chooses the smaller seniority) is dominated by the upstream seniority, scaling as in eq 32. This scaling is illustrated in Figure 5a, where the seniority distribution is calculated for a branching probability of $b^U = 0.4999$.

The distribution of relaxation times for polymers produced via the metallocene chemistry is hence different to that of a standard gelation ensemble, where $s_m \sim m^{-3}$ (this latter scaling may be obtained by assuming that both up and downstream directions are identical, having the scaling of eq 32, then using eq 27).

The difference in the asymptotic behavior of the seniority distribution in the two cases of metallocene LCB and gelation may be significant insofar as it affects the contribution of the high-seniority tail to the viscosity. The continuous extension of the Ball–McLeish equation (eq 2) for the relaxation time τ_m of a segment of seniority m is

$$\frac{d(\ln \tau)}{dm} = \nu \tilde{N}_x S_m^\alpha \quad (33)$$

where $\nu = 15/4$ and $\tilde{N}_x = N_x/N_e$ is the number of entanglements between branch points. If we choose a power-law tail for the unrelaxed concentration at seniority m , so $S_m \sim m^{-\sigma}$, then we see that $\alpha\sigma = 1$ corresponds to a critical point: for $\alpha\sigma \leq 1$, then the maximum relaxation time diverges with the seniority

(we may imagine a series of ensembles in which a cutoff to the power-law distribution is continuously increased), otherwise the relaxation time given by the BM equation tends to a limit for arbitrarily large seniority. This case is indicative of a “disentanglement transition”—the longest connected paths would actually relax via a slow Rouse-like process, but this would not be exponentially longer than the longest relaxation time dominated by entangled arm retraction.²⁸

From the above discussion, we find $\sigma = 1$ for the LCB metallocene process, and we recall that $\alpha = 4/3$. The practical consequence of this result is that as b^U tends to 0.5, the maximum relaxation time is only weakly convergent. We also note that, as in Figure 5a, the distribution at low seniorities approaches the $\sigma = 1$ power law limit *from below*: the apparent value of σ near seniorities of order 20 is closer to 0.7.

The true situation is best illustrated by numerical evaluation of the relaxation times in the Ball–McLeish equation (eq 2). Figure 6a shows the relaxation time as a function of seniority for $\bar{N}_x = 5.0$ and a range of branching probabilities (in all curves, $\tau(m = 1)$ is set to 1). Figure 6b gives the equivalent result for the gelation ensemble, and Figure 6c compares the terminal times as a function of branching probability of the two ensembles. While the terminal time of the metallocene ensemble does (eventually) converge as the percolation limit of $b^U = 0.5$ is approached, for most practical purposes the terminal time is apparently divergent. The cutoff to the seniority distribution directly controls the longest relaxation time, and hence the viscosity, of the melt. It is not possible to allow the branching probability b^U to tend arbitrarily close to 0.5, despite the possible motivation to do so from the benefit of including the concomitant high priorities in the distribution (these would provide strong extension-hardening, for example). However, in the case of the gelation ensemble (pure random branching in either direction along the molecule), the result $\sigma = 2$ permits arbitrary extension of the tail in seniority (and priority) *without penalty to the zero shear viscosity*, and this is illustrated well by the numerical results of Figure 6b. We note that the gelation ensemble is a candidate model for standard low-density polyethylene. Hence, these observations may be relevant to the qualitative difference between the extensional rheology of LDPE and metallocene LCB melts.

4.2. The Priority Distribution. The priority of a given strand in a polymer chain may be calculated by counting the number of free ends attached in the upstream and downstream directions, then taking the smaller value from the two directions. As in the case of seniority, it is convenient first to calculate the two “single-sided” distributions (i.e., the number of free ends upstream and downstream) before combining them to form the “bidirectional” distribution of priorities found from the smaller of the upstream and downstream priorities.

The easiest method for calculating priorities is by means of generating functions.^{29,32} Suppose the probability of a strand chosen at random having priority k upstream is p_k^U . Then, we define the upstream generating function as this polynomial:

$$F^U(z) = \sum_{k=1}^{\infty} p_k^U z^k \quad (34)$$

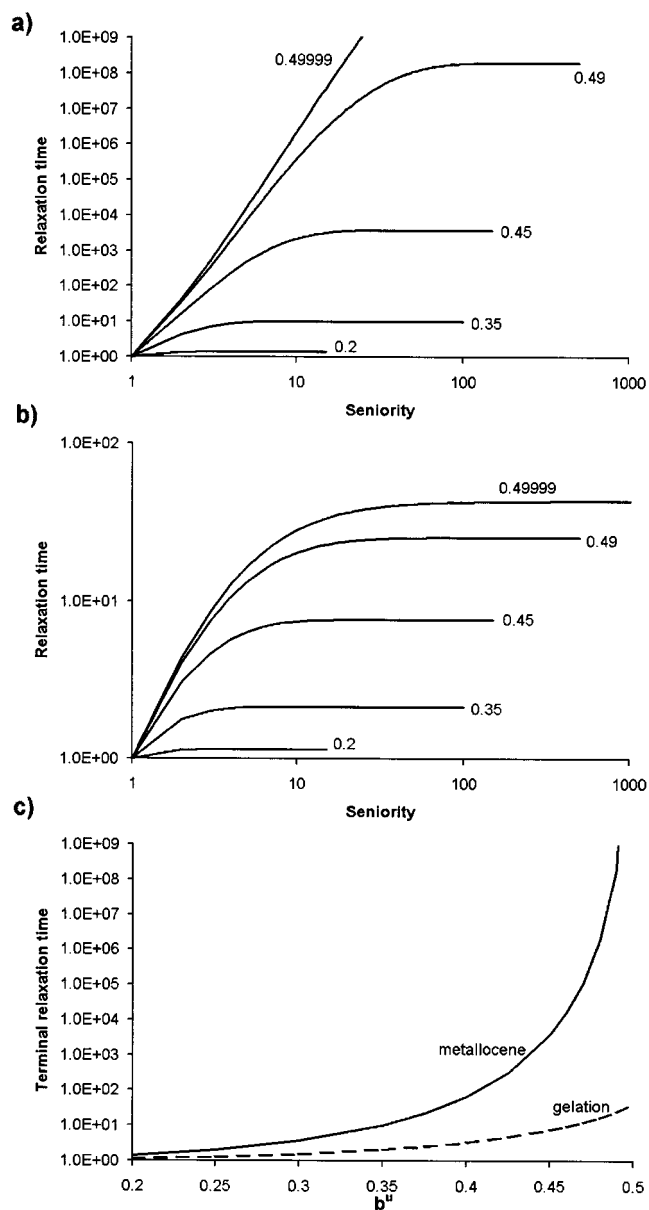


Figure 6. Orientational relaxation time vs seniority as calculated using the Ball–McLeish formula, with $\bar{N}_x = 5.0$ and $\tau(1) = 1$: (a) metallocene ensemble, at various values of the branching probability $b^U = 0.2, 0.35, 0.45, 0.49, 0.49999$; (b) gelation ensemble, at the same values of branching probability; (c) terminal relaxation time vs branching probability for the two ensembles.

Since all strands have the same probability distribution, they all have the same generating function. Any given strand will either be unbranched (priority 1, with probability b^U), or will be branched, with probability b^U . If it is branched, then its upstream priority is the sum of the priorities of the two subsequent strands. The probability weights for possible values of this sum are neatly captured as the coefficients of z^k in the product $[F^U]^2$. Therefore, a self-consistent formula for F^U is

$$F^U = (1 - b^U)z + b^U[F^U]^2 \quad (35)$$

This formula is quadratic in F^U and may readily be solved and expanded in powers of z , yielding

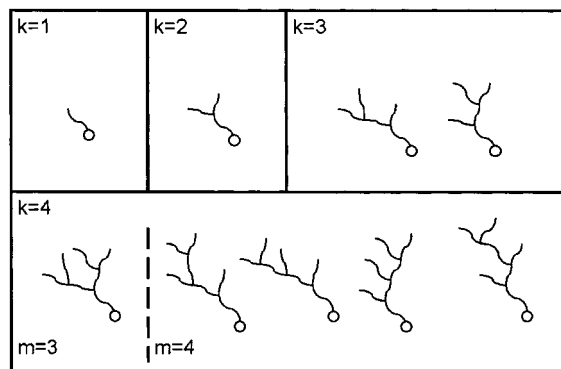


Figure 7. Illustration of the set of molecular shapes giving rise to (single sided) priorities of $k = 1, 2, 3,$ and 4 . The number of cases for each priority is given by the combinatorial factor $(2k-2)!/k!(k-1)!$. Each set of priorities may be divided into subsets of different seniorities, the number in each subset being given by $g_{k,m}^U - g_{k,m-1}^U$.

$$F^U = \frac{1 - \sqrt{1 - 4b^U(1 - b^U)z}}{2b^U} \quad (36)$$

$$= \sum_{k=1}^{\infty} z^k \frac{(2k-2)!}{k!(k-1)!} (b^U)^{k-1} (1 - b^U)^k \quad (37)$$

from which can easily be read the probabilities p_k^U . Note that these probabilities contain the product $(b^U)^{k-1} (1 - b^U)^k$. This is a direct consequence of the fact that any (sub)branch with priority k contains k free ends and $k - 1$ branch points. The numerical prefactor $(2k - 2)!/k!(k - 1)!$ is simply the combinatorial weight of all such branches, as is illustrated for the first few combinations in Figure 7.

The downstream priority distribution may be obtained by similar reasoning, from a downstream generating function

$$F^D(z) = \sum_{k=1}^{\infty} p_k^D z^k \quad (38)$$

Since there is one upstream and one downstream branch after a branchpoint, we find

$$F^D = (1 - b^D)z + b^D F^D F^U \quad (39)$$

and hence (making use of eq 36) we obtain

$$F^D = \frac{(1 - b^D)z}{\sqrt{1 - 4b^U(1 - b^U)z}} \quad (40)$$

$$= \sum_{k=1}^{\infty} z^k \frac{(2k-2)!}{(k-1)!^2} (b^U)^{k-1} (1 - b^U)^{k-1} (1 - b^D) \quad (41)$$

This time, the probabilities all contain the product $(b^U)^{k-1} (1 - b^U)^{k-1} (1 - b^D)$; a downstream branch with priority k has one downstream termination (the single free end with the P, D⁻, or D group) and $k - 1$ upstream terminations. The $k - 1$ branchpoints may be approached from upstream (probability b^U) or downstream (probability $b^D = 2b^U$), but the factors of 2 from the downstream branches are absorbed into the numerical prefactor $(2k-2)!/(k-1)!^2$.

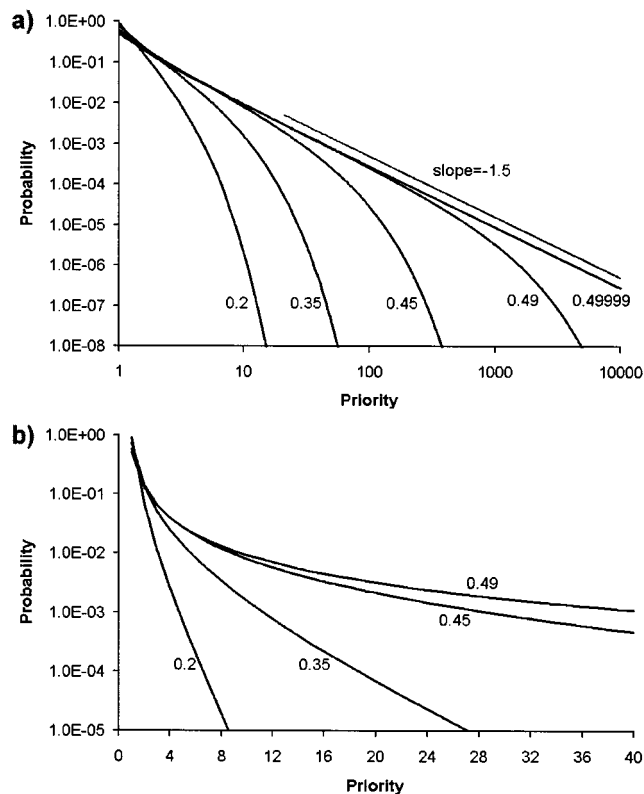


Figure 8. Priority distribution p_k for different values of the branching parameter, $b^U = 0.2, 0.35, 0.45, 0.49, 0.49999$ on (a) a log-log scale and (b) a linear-log scale. There is a crossover between exponential decay and power-law dominated behavior—the power law dominates for lower priorities and close to the percolation threshold.

Since the maximum stretch of a chain segment is limited by the branchpoint that can support the smallest maximum force, the bidirectional priority is always the smaller of the upstream and downstream priorities. Hence, a bidirectional priority of k is obtained when the upstream priority equals k and the downstream priority $> k$, or when the downstream priority equals k and the upstream priority $> k$, or when both equal k . In terms of probabilities, this reads

$$p_k^B = p_k^U p_k^D + p_k^U \sum_{k'=k+1}^{\infty} p_{k'}^D + p_k^D \sum_{k'=k+1}^{\infty} p_{k'}^U \\ = p_k^U [1 - \sum_{k'=1}^{k-1} p_{k'}^D] + p_k^D [1 - \sum_{k'=1}^{k-1} p_{k'}^U] - p_k^U p_k^D \quad (42)$$

Figure 8 shows the priority distribution for various values of b^U . The most branched ensemble is reached at the “gel point” of $b^U = 1/2$. At this point, just as in the case of the randomly branched ensemble,²⁹ the distributions take on power-law forms. In our case the priority distribution is dominated by the upstream value (the downstream cluster is typically very much more branched), and is less convergent than in random branching. By using Stirling’s approximation³¹ on p_k^U , we find $p_k^B \sim k^{-3/2}$ rather than the k^{-2} found for random branching.

4.3. Bivariate Distribution of Seniority and Priority. We noted above that the probability of obtaining a given priority was expressed as a product of a combinatorial integer, and a product of probabilities (for

example, upstream this was $(b^U)^{k-1}(1 - b^U)^k$ representing k free ends and $k - 1$ branch points). As illustrated in Figure 7 for priority $k = 4$, the set of molecular shapes with a given priority can be grouped into subsets with different seniorities, m . It must therefore be the case that the seniority distributions given above can be expanded as

$$f_m^U = \sum_{k=1}^{\infty} g_{k,m}^U (b^U)^{k-1} (1 - b^U)^k \quad (43)$$

$$f_m^D = \sum_{k=1}^{\infty} g_{k,m}^D (b^U)^{k-1} (1 - b^U)^{k-1} (1 - b^D) \quad (44)$$

where $g_{k,m}^U$ is the number of possible branching combinations with priority k and seniority $\leq m$. These numbers are just generators of the bivariate distribution of seniority and priority that we seek! $g_{k,m}^D$ is also a combinatorial factor, but includes factors of 2 to account for downstream, instead of upstream, branches. $g_{k,m}^U$ and $g_{k,m}^D$ are integers, independent of the branching probability b^U .

These two expansions may be substituted into the eqs 25 and 26 for the seniority distributions, and terms with equal factors of $(b^U)^{k-1}(1 - b^U)^k$ or $(b^U)^{k-1}(1 - b^U)^{k-1}(1 - b^D)$ equated, yielding

$$g_{k,m}^U = \sum_{k'=1}^{k-1} g_{k',m-1}^U g_{k-k',m-1}^U \quad \forall \{m > 1, k > 1\} \quad (45)$$

$$g_{k,m}^D = 2 \sum_{k'=1}^{k-1} g_{k',m-1}^D g_{k-k',m-1}^D \quad \forall \{m > 1, k > 1\} \quad (46)$$

$$g_{1,m}^U = 1, g_{1,m}^D = 1 \quad \forall m \quad (47)$$

$$g_{k,1}^U = 0, g_{k,1}^D = 0 \quad \forall k > 1 \quad (48)$$

These four equations may be used to generate the full set of coefficients for eqs 43 and 44. The bivariate probability of seniority m and priority k is then (upstream, downstream and bidirectional)

$$w_{k,m}^U = (g_{k,m}^U - g_{k,m-1}^U) (b^U)^{k-1} (1 - b^U)^k \quad (49)$$

$$w_{k,m}^D = (g_{k,m}^D - g_{k,m-1}^D) (b^U)^{k-1} (1 - b^U)^{k-1} (1 - b^D) \quad (50)$$

$$w_{k,m}^B = w_{k,m}^U \sum_{\substack{k' \geq k \\ m' \geq m}} w_{k',m'}^D + \sum_{m' > m} w_{k,m'}^U \sum_{k' \geq k} w_{k',m'}^D + \sum_{k' > k} w_{k',m}^U \sum_{\substack{m' \geq m \\ m' > k}} w_{k',m'}^D + w_{k,m}^D \sum_{\substack{k' > k \\ m' > m}} w_{k',m'}^U \quad (51)$$

The bivariate distribution of seniority and priority, $w_{k,m}^B$ is plotted in Figure 9 for $b^U = 0.46$. A logarithmic scale for probabilities is chosen because it has been found^{22,23} that fractions of polymer as low as 10^{-5} can contribute significantly to the calculated rheology. This is especially true when the seniority (which controls relaxation times) and priority (controlling maximal stretches) are high.

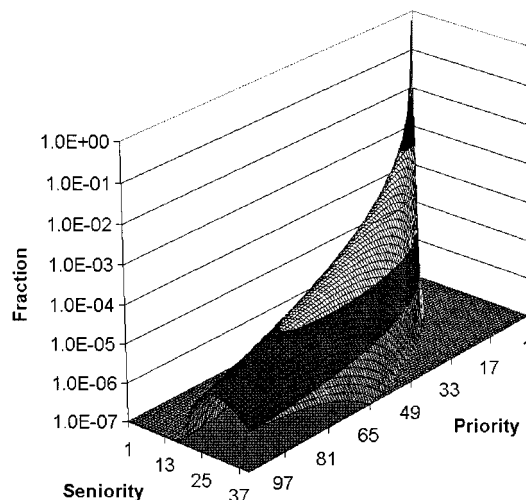


Figure 9. Bivariate distribution of seniority and priority for branching parameter $b^U = 0.46$.

Note that priorities are always larger than seniorities, with $m \leq k \leq 2^{m-1}$. The lower limit for k corresponds to segments on comblike structures, i.e., a “backbone” chain with single chain strands from each branchpoint. The upper limit for k corresponds to segments on Cayley tree structures, in which all chain segments within $m - 1$ steps of the original are branched. Of course, both limiting cases are unlikely, and the majority of chains are intermediate between the two limits.

4.4. Priority and Seniority as a Function of Relaxation Time: “Snipping”. We now consider the effect of constant flow at a given time scale or (equivalently) relaxation for a given time after a step strain. In these situations, there is a relaxation of all chain segments with a seniority less than that appropriate for the experimental time scale. They can no longer be considered as constrained by the polymer tubes, and therefore contribute little to the stress. Furthermore, they should not be included in the sum over all chain ends which gives the priority, since they carry no tension along the tube. It is as though these chain segments are “snipped” from the polymer molecules. We should recalculate the priority and seniority distributions accordingly.

Suppose that all segments with seniority $\leq n$ are “snipped”. In this case, the probability of a segment being snipped from upstream is f_n^U and from downstream it is f_n^D . The snipped chains have a typical form as shown in Figure 2. The new “free ends” are old branch points where both subsequent segments are snipped. The probability that a segment ends in a “free end” is thus s_{n+1}^U upstream and s_{n+1}^D downstream. These probabilities figure heavily in the results that follow.

The overall seniority distribution is unchanged, merely shifted by n units, so that the new probability of a segment having seniority m is

$$\tilde{s}_m^B = s_{m+n}^B \quad (52)$$

Details of the calculation of the priority and bivariate distributions after snipping are given in Appendix A. The methodology is very similar to the calculation without snipping. Here we present only the main results.

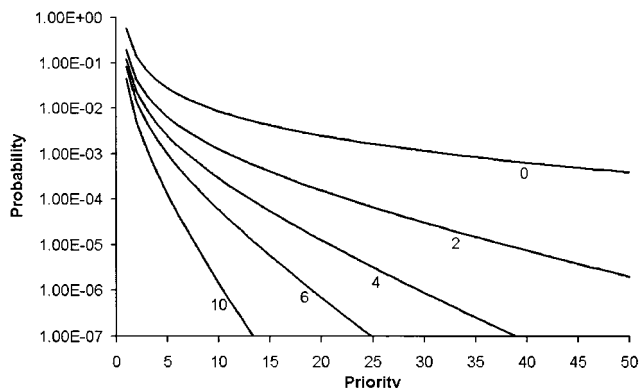


Figure 10. Effect of “snipping” (i.e., relaxation of low-seniority segments) on the effective priority distribution for $b^U = 0.46$ and snipping level $n = 0, 2, 4, 6, 10$.

The upstream distribution of priorities is

$$p_{n,k}^U = \frac{(2k - 2)!}{k!(k - 1)!} \frac{(s_{n+1}^U)^k (b^U)^{k-1}}{(1 - 2b^U f_n^U)^{2k-1}} \quad \forall k > 0$$

$$p_{n,0}^U = f_n^U \quad (53)$$

The downstream priority distribution is

$$p_{n,k}^D = \frac{(2k - 2)!}{(k - 1)!^2} \frac{s_{n+1}^D (s_{n+1}^U b^U)^{k-1}}{(1 - 2b^U f_n^U)^{2k-1}} + \frac{2(2k - 1)!}{k!(k - 1)!} \frac{f_n^D (s_{n+1}^U b^U)^k}{(1 - 2b^U f_n^U)^{2k}} \quad \forall k > 0$$

$$p_{n,0}^D = f_n^D \quad (54)$$

The “bidirectional” distribution is calculated analogously to eq 42. The effect of snipping on the priority distributions is illustrated in Figure 10, in which distributions are calculated for $b^U = 0.46$ and $n = 0, 2, 4, 6$ and 10 . Note that, while snipping merely shifts the seniority distribution by n along the seniority axis, it results in a drastic decrease in the effective priority.

For the unsnipped bivariate distributions, probabilities were expanded in terms of “branching” and “termination” events. The expansion in the case of snipping is in terms of similar events, illustrated in Figure 13 (in Appendix A), including side branches which are “snipped”. The probabilities of these events are written as

$$p_{1,n} = \frac{s_{n+1}^U}{(1 - f_n^U)} \quad (55)$$

$$p_{2,n} = 2b^U f_n^U \quad (56)$$

$$p_{3,n} = b^U (1 - f_n^U) \quad (57)$$

$$p_{a,n} = \frac{s_{n+1}^D}{(1 - f_n^D)} \quad (58)$$

$$p_{c,n} = 2b^U f_n^D \frac{(1 - f_n^U)}{(1 - f_n^D)} \quad (59)$$

from which the snipped upstream and downstream bivariate distributions are found as

$$\tilde{w}_{k,m,n}^U = \sum_{l=0}^{\infty} (g_{k,l,m}^U - g_{k,l,m-1}^U) p_{1,n}^k p_{3,n}^{k-1} p_{2,n}^l \quad (60)$$

and

$$\tilde{w}_{k,m,n}^D = \sum_{l=0}^{\infty} (g_{k,l,m}^D - g_{k,l,m-1}^D) p_{a,n} p_{1,n}^{k-1} p_{3,n}^{k-1} p_{2,n}^l + \sum_{l=0}^{\infty} (h_{k,l,m}^D - h_{k,l,m-1}^D) p_{c,n} p_{1,n}^k p_{3,n}^{k-1} p_{2,n}^l \quad (61)$$

So, in this case, the natural generators of the distribution $g_{k,l,m}$ and $h_{k,l,m}$ count not only priority k and seniority m , but also the number of entirely diluted (snipped) side branches, l . The numerical coefficients are generated from

$$g_{k,l,m}^U = g_{k,l-1,m-1}^U + \sum_{k'=1}^{k-1} \sum_{l'=0}^l g_{k',l,m-1}^U g_{k-k',l-l',m-1}^U \quad \forall \{m > 1, (k > 1 \text{ or } l > 0)\} \quad (62)$$

$$g_{1,0,m}^U = 1, \quad \forall m \quad (63)$$

$$g_{k,l,1}^U = 0, \quad \forall k > 1 \text{ or } l > 0 \quad (64)$$

and

$$g_{k,l,m}^D = g_{k,l-1,m-1}^D + 2 \sum_{k'=1}^{k-1} \sum_{l'=0}^l g_{k',l,m-1}^U g_{k-k',l-l',m-1}^D \quad \forall \{m > 1, (k > 1 \text{ or } l > 0)\} \quad (65)$$

$$h_{k,l,m}^D = h_{k,l-1,m-1}^D + g_{k,l,m-1}^U + 2 \sum_{k'=1}^{k-1} \sum_{l'=0}^l g_{k',l,m-1}^U h_{k-k',l-l',m-1}^D \quad \forall \{m > 1\} \quad (66)$$

$$g_{1,0,m}^D = 1, \quad \forall m \quad (67)$$

$$g_{k,l,1}^D = 0, \quad \forall k > 1 \text{ or } l > 0 \quad (68)$$

$$h_{k,l,1}^D = 0, \quad \forall k, l \quad (69)$$

“Bidirectional” distributions, $\tilde{w}_{k,m,n}^B$ from the smallest seniority and priority from upstream and downstream, are found from an equation analogous to eq 51. Examples of these distributions, for $b^U = 0.46$ and $n = 2$ and 4 are shown in Figure 11. The upper priority limit of $k \leq 2^{m-1}$ is preserved (on snipping from a Cayley tree, the seniority is decreased by n but the priority is divided by a factor 2^n). However, the lower limit of $k \geq m$ no longer holds (on snipping from a comb, the priorities of remaining segments are all immediately reduced to one). Again, the true behavior is intermediate between the two limits, though perhaps closer to the comblike limit.

Clearly “snipping” results in a drastic reduction of the typical priority at a given seniority (compare Figure 11

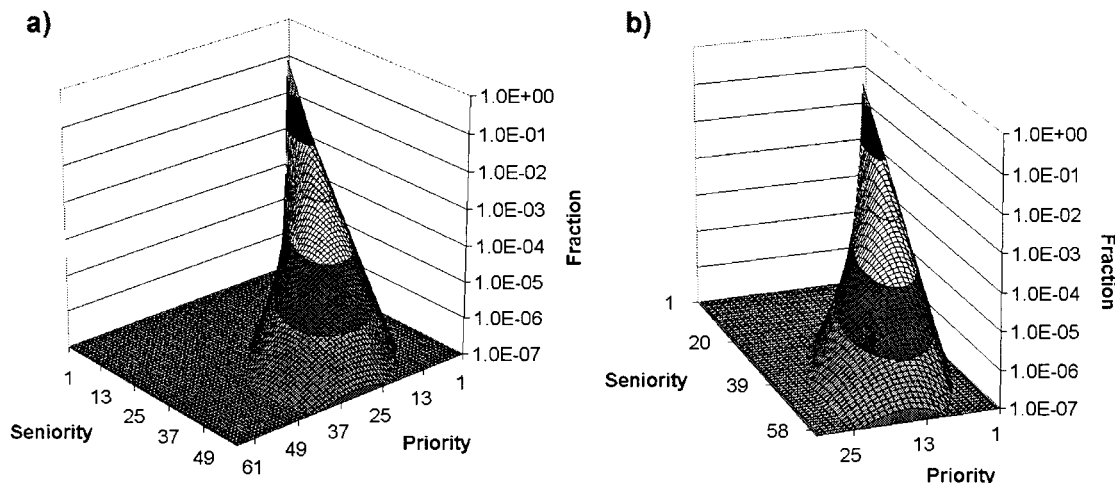


Figure 11. Effect of “snipping” (i.e., relaxation of low-seniority segments) on the bivariate distribution of seniority and priority for $b^U = 0.46$ and snipping level (a) $n = 2$ and (b) $n = 4$.

to the “unsnipped” case of Figure 9). The physical interpretation is as follows: we are considering flow at a given time scale, in which the outer segments of the polymers are relaxed from their tubes. In this case the maximal stretch of inner chain segments is much less than would be predicted from the “literal” priority, i.e., from counting the number of chemical chain ends of the polymers, as in Figure 1b. Instead, the maximal stretch depends on the time scale of the flow and corresponds to the number of “physical” chain ends created by relaxation of the outer segments. This “maximal stretch” of chain segments between branch points is a fundamental part of branched polymer constitutive modeling, contributing to the limit of extensional hardening of the polymer melt.

5. Decoupling Predictions of Rheology

We now illustrate how nontrivial rheological response may be calculated using the procedure outlined in section 2 above, mapping the essentially trivariate distribution for priorities and seniorities $\tilde{w}(k, m, n)$ onto a multimode pom-pom ensemble. In a full calculation of this approximation to the melt rheology, the coupling between molecular segments at different levels is ignored so that, for a flow rate setting the value of n , each population of priority and seniority is represented by a single pom-pom mode^{21,22} of orientation time $\tau_b(m)$ and maximum stretch k , with a contribution to the total stress proportional to its statistical weight. In this first calculation we further approximate the rheological model by limiting each seniority m to a single pom-pom mode, with a priority \bar{k} calculated as the weighted average of all priorities at the corresponding time scales of structure (m) and flow (n). For all ensembles, the sum over seniorities and their associated pom-pom modes was cut off when their statistical weights fell below 10^{-5} . In light of these approximations, we stress that the following results represent only a preliminary investigation into the calculation of metallocene LCB polymer rheology; we defer a more detailed study to a future work.

We review briefly the equation set for pom-pom modes. The essential physics captured by this formalism is that entangled chain segments have distinct relaxation times (and processes) for their stretch and orientation. First, the orientation of the mode is described by the tensorial second-moment average of the segmental orientation

distribution $\mathbf{S}(k, m, t)$. This has unit trace, by definition, and is given by $\mathbf{S}(k, m, t) = \mathbf{A}(k, m, t)/\text{trace}(\mathbf{A})$, where

$$\frac{D\mathbf{A}}{Dt} = \mathbf{K} \cdot \mathbf{A} - \mathbf{A} \cdot \mathbf{K}^T - \frac{1}{\tau_b(m)} \left(\mathbf{A} - \frac{\mathbf{I}}{3} \right) \quad (70)$$

A separate dynamical equation is obeyed by the stretch $\lambda(k, m, t)$ of the pom-pom mode:

$$\frac{D\lambda}{Dt} = [\mathbf{K} : \mathbf{S}(k, m, t)]\lambda - \frac{e^{(\nu/k)(\lambda-1)}}{\tau_s(m)} (\lambda - 1) \quad \lambda \leq k \quad (71)$$

The derivative D/Dt is the total convective derivative of fluid mechanics. When the stretch dynamics would attempt to give a value greater than k (the maximum stretch), λ is simply held at k . This is the consequence of “branch point withdrawal” as discussed in section 2.

The hierarchy of orientational relaxation times $\tau_b(m)$ is calculated from the Ball–McLeish equation (eq 2), starting with the smallest time scale of the first retracting arm using star–polymer theory. The fundamental time scale is set by a choice for the Rouse time of a single entanglement strand τ_e . Similarly, the fundamental degree of polymerization is that corresponding to a single entanglement, so we normalize the degree of polymerization between branchpoints as $\tilde{N}_x = N_x/N_e$. The stretch time scales are importantly shorter than the orientational times: they are effectively the attempt times for the orientational relaxation of the next highest seniority, so we set $\tau_s(m) = \tau_b(m+1)[\tilde{N}_x S(m)]^2$. The important exponential nonlinearity in the stretch equation accounts for the reduction of effective relaxation times when branch points are withdrawn into tubes of deeper segments as the molecule is strained. The mobility is reduced for higher priority segments as k^{-1} , and the value of ν found in experiments on H-polymers¹⁶ and in fitting to LDPE²² is 2. Some care needs to be taken over the existence of a sizable fraction of linear polymers that relax by reptation rather than fluctuation. These are handled by ascribing their weight to a pom-pom mode with no propensity to stretch at all (constant contour length), and with an orientational relaxation time of $\tau_{\text{rept}} = \tau_e \tilde{N}_x^3$.

Parts a and b of Figure 12 show the computed transient extensional stress growth for two architectures, of b^U values 0.2 and 0.46, but with \tilde{N}_x varied so

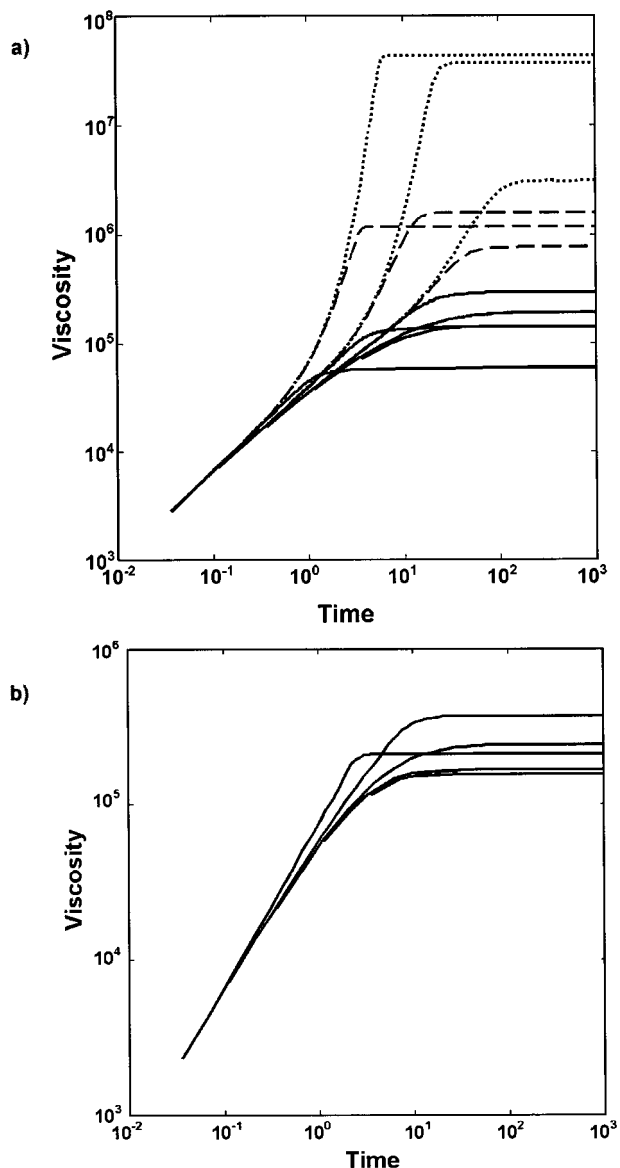


Figure 12. Extensional stress-growth coefficients computed for model metallocene polyethylene ensembles with (a) $b^U = 0.46$ and $\bar{N}_x = 2.7$ and (b) $b^U = 0.2$ and $\bar{N}_x = 9.5$. \bar{N}_x is chosen so that $\eta_0 \approx 10^5$ Pa in both cases. Extension rates are 1.0, 0.3, 0.1, 0.03, 0.01, and 0.03 s^{-1} . For the case of $b^U = 0.46$ snipping levels of $n = 0$ (dots), 2 (dashes), and 10 (solid curve) are shown. The first two snipping levels are, in fact, unphysical at these strain rates.

that zero shear viscosities are comparable. For $b^U = 0.2$ we used $\bar{N}_x = 9.5$, but keeping a similar viscosity in the more highly branched ensemble ($b^U = 0.46$) requires a much smaller $\bar{N}_x = 2.7$ so that the molecules are more compact. Values of τ_e and G_0 suitable for polyethylene at 190 °C were chosen.

For the more highly branched architecture (Figure 12a) we have computed the strain hardening for “snipping” degrees of $n = 0, 2,$ and 10 for the extension rate range of 10^{-2} to 1 s^{-1} . “Snipping” represents a simplification of the effective topological structure of the molecules, imposed by dynamic dilution. Clearly, snipping is very effective indeed at reducing the extension hardening at values of b^U as high as 0.46 . Of course, the physically-realized stress-growth curves are those that correspond to equated flow and snipping time scales: $\tau(m = n) = \dot{\epsilon}$. At the flow-rates actually com-

puted of $\dot{\epsilon} \lesssim 1$ s^{-1} , the physical values of n required in the $b^U = 0.46$ case are in the range 10 – 20 ! The extreme hardening of 3 orders of magnitude seen in the $n = 0$ case would physically only be observed at much higher flow rates than these ($\gtrsim 10^4$ s^{-1}) because of the small relaxation times of the short outer segments in these architectures. However, for $b^U = 0.2$ the larger degree of polymerization between branchpoints gives a larger relaxation time at a given seniority, so that the un-snipped ensemble ($n = 0$) shown in Figure 12b is actually the relevant one. Dynamic dilution induced “snipping” becomes more important as the flow rate changes for higher degrees of branching.

The hardening observed in the more branched ensemble at higher rates is clearly much greater than at the (chemically more practical) values of $b^U \sim 0.2$. However, if we keep the viscosity constant, in mildly nonlinear response the extensional stress growth is almost independent of degree of branching (compare the $n = 10$ curve of Figure 12a with Figure 12b)! The practical effect of increasing the level of branching in metallocene LCB polymers is to enhance the amount of hardening at the highest rates only. This is connected with our earlier observation that the terminal time (and hence viscosity) is typically a strong function of b^U for the metallocene ensemble. The natural consequence is a necessity for a strong reduction of N_x to maintain constant viscosity with increasing b^U , and the strong degree of “snipping” follows. A practical limit to the extension-hardening parameter of ~ 3 seems to hold.

6. Conclusions

We have found that the ensemble of branched polymers generated by the single site metallocene chemistry can be calculated as a two-parameter family. Convenient parameters for this family are the probability of encountering a branchpoint moving “upstream” within a molecule, b^U , and the average molecular weight between branch points N_x . The parameters may themselves be linked directly to reaction constants and concentrations for the polymerization.

These tools, together with recursion relations and generating functions, may be employed to calculate the bivariate weights of the rheologically relevant statistics of seniority and priority, when an arbitrary amount of the molecule has been removed from the entanglement ensemble by dynamic dilution. The asymptotics for these distributions indicate that the LCB metallocene ensemble differs qualitatively from pure random branching (which may be a reasonable approximation to LDPE). In particular, the high tail of the distribution in both seniority and priority is much larger in the metallocene case. This leads to unacceptably high viscosities when very high branching is generated unless the molecular weight between branch points is kept very low. This in turn limits the degree of strain hardening that can be produced in practice.

Mapping the bivariate distribution onto decoupled “pom-pom” constitutive elements permits prediction of transient extension hardening curves as a function of the molecular parameters. In our preliminary investigations, extension hardening is seen over a wide range of extension rates, but similar values to those found in LDPE are in principle attainable only at flow rates that diverge with the required degree of hardening. In mildly nonlinear flows we conjecture that the maximum ex-

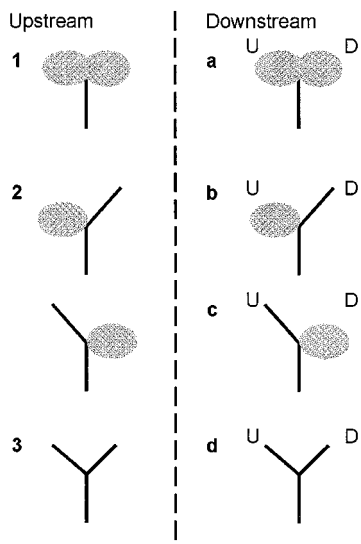


Figure 13. Possible arrangements following an unsnippeted strand in the upstream and downstream directions. In the upstream direction, we have (1) both subsequent strands snipped, (2) one subsequent strand snipped, or (3) neither subsequent strand snipped. In the downstream direction, we need to distinguish between the subsequent up (U) and downstream (D) strands.

tension hardening at dimensionless extension rates $\dot{\epsilon}\tau_{\max} \approx 10-100$ is roughly independent of architecture and limited to ~ 3 . Careful rheological experiments on well-characterized ensembles are strongly suggested, but may require a much more sophisticated treatment of the structure rheology relationship.

Appendix A. Calculation of Distributions after Snipping

A.1. Priority Distribution after Snipping. As before, we generate the priority distribution upstream and downstream using the generating function method, and calculate the bidirectional distribution from these. We start with the upstream generating function, defined as

$$F_n^U(z) = \sum_{k=1}^{\infty} p_{n,k}^{cU} z^k \quad (72)$$

where $p_{n,k}^{cU}$ is the probability that a segment has upstream priority k at snipping level n , subject to the condition that this segment has not itself been “snipped”. $p_{n,k}^{cU}$ is related to the unconditional probability of priority k (i.e., inclusive of all snipped and unsnippeted segments) via

$$\begin{aligned} p_{n,k}^U &= (1 - f_n^U) p_{n,k}^{cU} \quad \forall k > 0 \\ p_{n,0}^U &= f_n^U \end{aligned} \quad (73)$$

Since all strands have the same statistics, we can (as before) write a self-consistent formulas for F_n^U . We note that there are three distinct possibilities for a strand, illustrated in Figure 13. It could either be followed by two snipped strands (probability $p_{1,n}$), one snipped strand (probability $p_{2,n}$) or by two unsnippeted strands (probability $p_{3,n}$). We derive these probabilities as follows; If the strand is followed by two snipped strands,

then its current seniority is 1, and its original seniority was $n + 1$. Therefore

$$p_{1,n} = \frac{s_{n+1}^U}{(1 - f_n^U)} \quad (74)$$

where the factor $(1 - f_n^U)$ is due to the condition that this segment has not itself been “snipped”.

If the strand is not followed by two snipped strands, then its original seniority must be greater than $n + 1$ and the conditional probability for this is

$$\frac{(1 - f_{n+1}^U)}{(1 - f_n^U)}$$

It also follows that the following two strands cannot *both* be snipped; the probability that one is snipped is therefore

$$p_{2,n} = \frac{(1 - f_{n+1}^U)}{(1 - f_n^U)} \times 2 \frac{(1 - f_n^U) f_n^U}{(1 - f_n^{U2})} = 2b^U f_n^U \quad (75)$$

and the probability that neither is snipped is

$$p_{3,n} = \frac{(1 - f_{n+1}^U)}{(1 - f_n^U)} \times \frac{(1 - f_n^U)^2}{(1 - f_n^{U2})} = b^U (1 - f_n^U) \quad (76)$$

where eq 25 has been used to simplify the expressions.

A self-consistent formula for F_n^U is thus

$$F_n^U = p_{1,n} z + p_{2,n} F_n^U + p_{3,n} (F_n^U)^2 \quad (77)$$

which may be solved to give

$$\begin{aligned} p_{n,k}^U &= \frac{(2k - 2)!}{k!(k - 1)!} \frac{(s_{n+1}^U)^k (b^U)^{k-1}}{(1 - 2b^U f_n^U)^{2k-1}} \quad \forall k > 0 \\ p_{n,0}^U &= f_n^U \end{aligned} \quad (78)$$

Similarly, downstream we can define an analogous conditional generating function

$$F_n^D(z) = \sum_{k=1}^{\infty} p_{n,k}^{cD} z^k \quad (79)$$

such that

$$\begin{aligned} p_{n,k}^D &= (1 - f_n^D) p_{n,k}^{cD} \quad \forall k > 0 \\ p_{n,0}^D &= f_n^D \end{aligned} \quad (80)$$

For a strand that has not been snipped from downstream, there are four downstream possibilities, illustrated in Figure 13. Both following strands could be snipped (probability $p_{a,n}$), just the upstream branch could be snipped (probability $p_{b,n}$), just the downstream branch could be snipped (probability $p_{c,n}$), or both strands could be unsnippeted (probability $p_{d,n}$). We find

$$p_{a,n} = \frac{s_{n+1}^D}{(1 - f_n^D)} \quad (81)$$

$$p_{b,n} = \frac{(1 - f_{n+1}^D)}{(1 - f_n^D)} \times \frac{(1 - f_n^D) f_n^U}{(1 - f_n^U f_n^D)} = 2b^U f_n^U \quad (82)$$

$$p_{c,n} = \frac{(1 - f_{n+1}^D)}{(1 - f_n^D)} \times \frac{(1 - f_n^U) f_n^D}{(1 - f_n^U f_n^D)} = 2b^U f_n^D \frac{(1 - f_n^U)}{(1 - f_n^D)} \quad (83)$$

$$p_{d,n} = \frac{(1 - f_{n+1}^D)}{(1 - f_n^D)} \times \frac{(1 - f_n^U) (1 - f_n^D)}{(1 - f_n^U f_n^D)} = 2b^U (1 - f_n^U) \quad (84)$$

and the formula for F_n^D is

$$F_n^D = p_{a,n} Z + p_{b,n} F_n^D + p_{c,n} F_n^U + p_{d,n} F_n^D F_n^U \quad (85)$$

from which we obtain

$$p_{n,k}^D = \frac{(2k-2)! s_{n+1}^D (s_{n+1}^U b^U)^{k-1}}{(k-1)!^2 (1 - 2b^U f_n^U)^{2k-1}} + \frac{2(2k-1)! f_n^D (s_{n+1}^U b^U)^k}{k!(k-1)! (1 - 2b^U f_n^U)^{2k}} \quad \forall k > 0$$

$$p_{n,0}^D = f_n^D \quad (86)$$

Note there are now two separate terms in the probability distribution. This represents the fact that, with snipping, there are two possible ways that the downstream series can be terminated. Either it will terminate by ending on a segment with both subsequent branches snipped (event *a* above), or it will terminate by ending on a segment where only the subsequent downstream branch is snipped (event *c* above). Each type of termination leads to a different set of possible combinations for the molecule, with different probability weightings, hence the two separate terms in the probability distribution. Note that the second term is zero in the limit of no snipping, where $f_n^D = 0$.

A.2. Bivariate Seniority/Priority Distribution after Snipping. We now aim to calculate the full bivariate distribution of seniority and priority after snipping. As in section 4.3, we recognize that all chain strands with a given priority *k* must be attached to *k* free ends and *k* - 1 branchpoints (in which neither subsequent branch is snipped). The difference after snipping is that there is an arbitrary number of branchpoints in which one of the subsequent branches are snipped.

In the upstream direction, we can equate a free end with event 1 in Figure 13; for priority *k* there are *k* of these. We can equate a "branch" with event 3 in Figure 13; for priority *k* there are *k* - 1 of these. There are an arbitrary number of event 2 at a given priority. Therefore, we can expand the cumulative upstream seniority distribution at snipping level *n* as

$$f_{n+m}^U = f_n^U + (1 - f_n^U) \sum_{k=1}^{\infty} \sum_{l=0}^{\infty} g_{k,l,m}^U p_{1,n}^k p_{3,n}^{k-1} p_{2,n}^l \quad (87)$$

where $g_{k,l,m}^U$ is the number of possible branching combinations with priority *k*, number of singly snipped branches *l*, and seniority $\leq m$. This expression may be substituted into the recursive formula for f_{n+m}^U

$$f_{n+m}^U = (1 - b^U) + b^U [f_{n+m-1}^U]^2 \quad (88)$$

and like terms with equal factors of $p_{1,n}^k p_{3,n}^{k-1} p_{2,n}^l$ equated, yielding

$$g_{k,l,m}^U = g_{k,l-1,m-1}^U + \sum_{k'=1}^{k-1} \sum_{l'=0}^l g_{k',l',m-1}^U g_{k-k',l-l',m-1}^U \quad \forall \{m > 1, (k > 1 \text{ or } l > 0)\} \quad (89)$$

$$g_{1,0,m}^U = 1, \quad \forall m \quad (90)$$

$$g_{k,l,1}^U = 0, \quad \forall k > 1 \text{ or } l > 0 \quad (91)$$

from which the full set of coefficients $g_{k,l,m}^U$ may be generated. The upstream bivariate seniority and priority distribution is then given by

$$\tilde{w}_{k,m,n}^U = \sum_{l=0}^{\infty} (g_{k,l,m}^U - g_{k,l,m-1}^U) p_{1,n}^k p_{3,n}^{k-1} p_{2,n}^l \quad (92)$$

In practice, the sum over *l* can be terminated at large finite *l* with little loss of accuracy, as extremely high values of *l* become exponentially improbable.

In the downstream direction, the situation is a little complicated by the fact that, with snipping, there are two possible ways that the downstream series can be terminated. Either it will terminate by ending on a segment with both subsequent branches snipped (event *a* above), or it will terminate by ending on a segment where only the subsequent downstream branch is snipped (event *c* above). In the former case, a strand with downstream priority *k* is attached to one free end which is an *a* event, *k* - 1 free ends which are type 1 events, *k* - 1 branches which are either type 3 or type *d*, and an arbitrary number of type 2 or type *b* singly snipped branches. In the latter case, a strand with downstream priority *k* is attached to *k* free ends which are type 1 events, *k* - 1 branches which are either type 3 or type *d*, an arbitrary number of type 2 or type *b* singly snipped branches and just one type *c* singly snipped branch. Furthermore, we note that $p_{d,n} = 2p_{3,n}$ and $p_{b,n} = p_{2,n}$ so we expand the downstream cumulative seniority as

$$f_{n+m}^D = f_n^D + (1 - f_n^D) \sum_{k=1}^{\infty} \sum_{l=0}^{\infty} [g_{k,l,m}^D p_{a,n} p_{1,n}^{k-1} p_{3,n}^{k-1} p_{2,n}^l + h_{k,l,m}^D p_{c,n} p_{1,n}^k p_{3,n}^{k-1} p_{2,n}^l] \quad (93)$$

where $g_{k,l,m}^D$ and $h_{k,l,m}^D$ are combinatorial factors which include factors of 2 from the fact that $p_{d,n} = 2p_{3,n}$. This expression may be substituted into the recursive formula for f_{n+m}^D

$$f_{n+m}^D = (1 - b^D) + b^D f_{n+m-1}^U f_{n+m-1}^D \quad (94)$$

and terms with equal factors of $p_{a,n} p_{1,n}^{k-1} p_{3,n}^{k-1} p_{2,n}^l$ or $p_{c,n} p_{1,n}^k p_{3,n}^{k-1} p_{2,n}^l$ equated, to give

$$g_{k,l,m}^D = g_{k,l-1,m-1}^D + 2 \sum_{k'=1}^{k-1} \sum_{l'=0}^l g_{k',l',m-1}^U g_{k-k',l-l',m-1}^D \quad \forall \{m > 1, (k > 1 \text{ or } l > 0)\} \quad (95)$$

$$h_{k,l,m}^D = h_{k,l-1,m-1}^D + g_{k,l,m-1}^U + 2 \sum_{k'=1}^{k-1} \sum_{l'=0}^l g_{k',l',m-1}^U h_{k-k',l-l',m-1}^D \quad \forall \{m > 1\} \quad (96)$$

$$g_{1,0,m}^D = 1, \quad \forall m \quad (97)$$

$$g_{k,l,1}^D = 0, \quad \forall k > 1 \text{ or } l > 0 \quad (98)$$

$$h_{k,l,1}^D = 0, \quad \forall k, l \quad (99)$$

from which the full set of coefficients $g_{k,l,m}^D$ and $h_{k,l,m}^D$ may be generated. The downstream bivariate seniority and priority distribution is then given by

$$\tilde{w}_{k,m,n}^D = \sum_{l=0}^{\infty} (g_{k,l,m}^D - g_{k,l,m-1}^D) p_{a,n} p_{1,n}^{k-1} p_{3,n}^{k-1} p_{2,n}^l + \sum_{l=0}^{\infty} (h_{k,l,m}^D - h_{k,l,m-1}^D) p_{c,n} p_{1,n}^k p_{3,n}^{k-1} p_{2,n}^l \quad (100)$$

Appendix B. Bivariate Distribution of Number of Branches and Degree of Polymerization

In ref 25, Soares and Hamielec derived an expression for the bivariate distribution of degree of polymerization and number of branches, using essentially the same reaction chemistry as described in the present work. We now show that one can derive exactly the same distribution using the principles in this paper, in particular the principle that the molecules are self-similar.

The probability distribution for the number of branches alone may be obtained directly from the upstream priority distribution evaluated in eq 37. If we start from the chain segment attached to the reactive end group, then the upstream priority k is just the total number of free ends in the upstream direction. The number of branches, β , is just $k - 1$, occurring with probability

$$P(\beta) = \frac{(2\beta)!}{\beta!(\beta+1)!} (b^U)^\beta (1 - b^U)^{\beta+1} \quad (101)$$

Given β branches, the number of chain strands is $2\beta + 1$. Note that each strand with a free end in the upstream direction must contain at least two monomers (since, with the prescribed reaction chemistry, the smallest two molecules that can form a branch are $P_{2,0}$ and $D_{2,0}$ —each containing two monomers and no branches). Therefore, the total molecular weight of a polymer chain is

$$N = 2(\beta + 1) + \sum_{i=1}^{2\beta+1} N_i \quad (102)$$

where N_i is the degree of polymerization of strand i and $N_i \geq 0$. We now need the probability distribution of the N_i , which can be found from a detailed balance argument. Suppose $[N_i]$ is the concentration of strands with degree of polymerization N_i . Then the kinetic equation for $[N_i]$ is, for $N_i > 0$

$$\frac{d[N_i]}{dt} = k_p M [N_i - 1] - k_p M [N_i] - k_{CTA} [CTA] [N_i] - k_\beta [N_i] - k_{pLCB} D^- [N_i] - s [N_i] \quad (103)$$

from which, in steady-state conditions, we obtain

$$[N_i] = A [N_i - 1] \quad (104)$$

where

$$A = \frac{k_p M}{\gamma} \quad (105)$$

$$\gamma = k_p M + k_{CTA} [CTA] + k_\beta + k_{pLCB} D^- + s \quad (106)$$

The normalized probability distribution for the N_i is

$$P(N_i) = A^{N_i} (1 - A) \quad (107)$$

Given β branches and $2\beta + 1$ chain strands, the probability distribution for N is therefore

$$P(N|\beta) = \frac{(N-2)!}{(N-2\beta-2)!(2\beta)!} A^{N-2(\beta+1)} (1-A)^{2\beta+1} \quad (108)$$

where the numerical prefactor represents the number of ways of distributing $N - 2\beta - 2$ monomers among $2\beta + 1$ strands. We obtain the bivariate probability distribution of degree of polymerization and number of branches as

$$P(N \cup \beta) = P(N|\beta) P(\beta) \cong \frac{N^{2\beta}}{\beta!(\beta+1)!} A^{N-2(\beta+1)} (1-A)^{2\beta+1} (b^U)^\beta (1-b^U)^{\beta+1} \quad (109)$$

where we have approximated $(N-2)!/(N-2\beta-2)!$ by $N^{2\beta}$.

A certain amount of simplification of this expression is possible. To obtain the expression in the form given by Soares and Hamielec, which was in terms of concentration $P_{N,\beta}$ of species with polymerization N and number of branches β , we note that

$$P_{N,\beta} = P(N \cup \beta) \times P \quad (110)$$

and hence

$$P_{1,0} = \frac{1-A}{A} (1-b^U) P \quad (111)$$

an expression which can be shown to be exactly equivalent to eq 10, a pleasing self-consistency in the formulas! Substituting back into eq 110 gives

$$P_{N,\beta} = \frac{N^{2\beta}}{\beta!(\beta+1)!} A^{N-(\beta+1)} C^\beta P_{1,0}^{\beta+1} \quad (112)$$

where

$$C = \frac{(1-A)b^U}{P} = \frac{k_{pLCB} k_\beta}{\gamma (k_{pLCB} D^- + s)} \quad (113)$$

Equation 112 is identical to eq 41 of ref 25. One must also comment on the striking similarity of eqs 101 and

109 to equations derived by Flory³³ for the condensation of AB and AB₂ monomers (where A can only react with B). In fact, the mean field statistical ensemble for the AB + AB₂ condensation chemistry is almost identical to that of the metallocene chemistry.

B.1. Continuum Representation and Molecular Weight Averages. Equation 108 can be cast in perhaps a more useful way by noting that it is approximately of the form

$$P(N|\beta) = \text{const} \times N^{2\beta} \exp(-N/N_x) \quad (114)$$

where $N_x = -1/\ln A$ is the mean length of a polymer strand between branches, and the normalization constant is found to be $1/[N_x^{2\beta+1}(2\beta)!]$. Equation 109 becomes

$$P(N \cup \beta) = \frac{N^{2\beta}}{N_x^{2\beta+1} \beta! (\beta + 1)!} (b^U)^\beta (1 - b^U)^{\beta+1} \exp(-N/N_x) \quad (115)$$

from which the various averages of degrees of polymerization may be calculated. The number-average degree of polymerization is

$$N_n = \frac{\sum_{\beta} \int [NP(N \cup \beta)] dN}{\sum_{\beta} \int [P(N \cup \beta)] dN} = \frac{N_x}{(1 - 2b^U)} \quad (116)$$

The weight-average degree of polymerization is

$$N_w = \frac{\sum_{\beta} \int [N^2 P(N \cup \beta)] dN}{\sum_{\beta} \int [NP(N \cup \beta)] dN} = \frac{2N_x(1 - b^U)}{(1 - 2b^U)^2} \quad (117)$$

Finally, the ratio of number of branchpoints to number of reacted monomers is

$$\varphi_b = \frac{\sum_{\beta} \int [\beta P(N \cup \beta)] dN}{\sum_{\beta} \int [NP(N \cup \beta)] dN} = \frac{b^U}{N_x} \quad (118)$$

References and Notes

- Quack, G.; Hadjichristidis, N.; Fetters, L. J.; Young, R. N. *Ind. Eng. Chem. Prod. Res. Dev.* **1980**, *19*, 587.
- Doi, M.; Edwards, S. F. *The Theory of Polymer Dynamics*; Oxford: Oxford, England, 1986.
- Metallocene-Catalyzed Polymers (Materials, Properties, Processing and Markets)*; Benedikt, G. M., Goodall, B. L., Eds.; Plastics Design Library, William Andrew Inc.: New York, 1998.
- Meissner, J. *Pure Appl. Chem.* **1975**, *42*, 551.
- Osaki, K.; Kurata, M. *Macromolecules* **1980**, *13*, 671.
- Rubinstein, M. *Phys. Rev. Lett.* **1987**, *59*, 1946. Deutsch, J. M.; Madden, T. L. *J. Chem. Phys.* **1989**, *91*, 3252. O'Connor, N. P. T.; Ball, R. C. *Macromolecules* **1992**, *25*, 5677.
- Doi, M.; Kuzuu, N. Y. *J. Polym. Sci., Polym. Lett. Ed.* **1980**, *18*, 775. Pearson, D. S.; Helfand, E. *Macromolecules* **1984**, *19*, 888. Ball, R. C.; McLeish, T. C. B. *Macromolecules* **1989**, *22*, 1911.
- For recent reviews see the chapters of: Rubinstein, M.; McLeish, T. C. B. In *Theoretical Challenges in the Dynamics of Complex Fluids*; McLeish, T. C. B., Ed.; Kluwer: Dordrecht, The Netherlands, 1997. McLeish, T. C. B.; Milner S. T. *Adv. Polym. Sci.* **1999**, *143*, 195.
- Fetters, L. J.; Kiss, A. D.; Pearson, D. S.; Quack, G. F.; Vitus, F. J. *Macromolecules* **1993**, *26*, 647.
- Milner, S. T.; McLeish, T. C. B. *Phys. Rev. Lett.* **1998**, *81*, 725.
- Milner, S. T.; McLeish, T. C. B. *Macromolecules* **1997**, *30*, 2159.
- Blottière, B.; McLeish, T. C. B.; Hakiki, A.; Young, R. N.; Milner, S. T. *Macromolecules* **1998**, *31*, 9295.
- Milner, S. T.; McLeish, T. C. B.; Johnson, J.; Hakiki, A.; Young, R. N. *Macromolecules* **1998**, *31*, 9345.
- Roovers, J. *Macromolecules* **1984**, *17*, 1196.
- McLeish, T. C. B. *Macromolecules* **1988**, *21*, 3639.
- McLeish, T. C. B.; Allgaier, J.; Bick, D. K.; Bishko, G.; Biswas, P.; Blackwell, R.; Blottière, B.; Clarke, N.; Gibbs, B.; Groves, D. J.; Hakiki, A.; Heenan, R.; Johnson, J. M.; Kant, R.; Read, D. J.; Young, R. N. *Macromolecules* **1999**, *32*, 6734–6758.
- Fetters, L. J.; Lohse, D. J.; Richter, D.; Witten, T. A.; Zirkel, A. *Macromolecules* **1994**, *27*, 4639.
- Osaki, K. *Rheol. Acta* **1993**, *32*, 429.
- Roovers, J.; Graessley, W. W. *Macromolecules* **1981**, *14*, 766.
- Yurasova, T. A.; McLeish, T. C. B.; Semenov, A. N. *Macromolecules* **1994**, *27*, 7205.
- McLeish, T. C. B.; Larson, R. G. *J. Rheol.* **1998**, *42*, 81.
- Inkson, N. J.; McLeish, T. C. B.; Groves, D. J.; Harlen, O. G. *J. Rheol.* **1999**, *43*, 873.
- Blackwell, R. J.; McLeish, T. C. B.; Harlen, O. G. *J. Rheol.* **2000**, *44*, 121.
- Soares, J. B. P.; Hamielec, A. C. *Polymer* **1995**, *36*, 2257.
- Soares, J. B. P.; Hamielec, A. C. *Macromol. Theory Simul.* **1996**, *5*, 547.
- Colby, R. H.; Rubinstein, M. *Macromolecules* **1990**, *23*, 2753.
- McLeish, T. C. B. *Europhys. Lett.* **1989**, *6*, 511.
- Rubinstein, M.; Zurek, S.; McLeish, T. C. B.; Ball, R. C. *J. Phys. (Fr.)* **1990**, *51*, 757.
- Bick, D. K.; McLeish, T. C. B. *Phys. Rev. Lett.* **1996**, *76*, 2587.
- Blackwell, R. J.; McLeish, T. C. B.; Harlen, O. G. *Macromolecules* **2000**, submitted.
- Note that for this calculation, it is necessary to use the first three terms of Stirling's approximation: $\ln n! \approx n \ln n - n + \frac{1}{2} \ln(2\pi n)$.
- de Gennes, P. G. *Scaling Concepts in Polymer Physics*; Cornell University Press: Ithaca, NY, 1979; pp 142–145.
- Flory, P. J. *Principles of Polymer Chemistry*; Cornell University Press: Ithaca, NY, 1953; Chapter IX-2b, eqs 19 and 30.

MA001483U